Int. J. Electrochem. Sci., 15 **(2020)** 10231 – 10242, doi: 10.20964/2020.10.72

International Journal of
ELECTROCHEMICAL
SCIENCE
www.electrochemsci.org

Short Communication

Preparation of chemically reduced graphene using hydrazine hydrate as the reduction agent and its NO_2 sensitivity at room temperature

Hao Chen[1,*], *Ling Ding*[1], *Kaibo Zhang*[1], *Zihao Chen*[2], *Yunlong Lei*[2], *Zigang Zhou*[2,*], *Ruonan Hou*[2]

[1] School of Material Science and Engineering, Southwest University of Science and Technology, Mianyang 621010
[2] School of Science, Southwest University of Science and Technology, Mianyang 621010
[*]E-mail: chenhao@swust.edu.cn, zhouzigang@swust.edu.cn

Received: 17 April 2020 / *Accepted:* 3 June 2020 / *Published:* 31 August 2020

Graphene oxide hydrogel was prepared from graphite oxide by a gel method and used as a precursor to obtain reduced graphene oxide (rGO) samples, which were prepared by reduction treatment of the graphene oxide (GO) using different levels of hydrazine hydrate dosage. The effects of hydrazine hydrate dosage on the structure, functional groups and gas-sensing properties of the GO samples were studied by means of X-ray diffraction (XRD), Raman spectroscopy (Raman), IR spectra (FT-IR) and a gas-sensing test. The results showed that with an increase in the amount of hydrazine hydrate, the oxygen-containing functional groups in the GO samples gradually disappeared, the degree of disorder (I_D/I_G) decreased from 1.59 to 1.22, and the resulting structure changed to a more orderly graphite-like structure. For a hydrazine hydrate dosage of 0.1 mL, GO was found to be almost completely reduced. The sensitivity of the samples to NO_2 detection showed a decreasing trend, while the response-recovery time showed an increasing trend. At room temperature, a sample prepared with a hydrazine hydrate dosage of 0.1 mL showed a static response sensitivity of 42.17%, response time of 123 s, and a recovery time of 295 s under a 100 ppm NO_2 environment.

Keywords: chemical reduction; rGO; room temperature; NO_2 detection

1. INTRODUCTION

In recent years, with much attention being paid to environmental governance in China and people's increasing awareness of pursuing a healthy life, real-time monitoring of toxic and harmful gases in the environment has received widespread attention. NO_2 is an air pollutant. At present, semiconductor metal oxide sensors are mainly used for NO_2 gas detection and have the characteristics of a relatively simple production process, stable performance and miniaturization [1-3]. The working

temperature for such sensors is generally approximately 200℃, which leads to high power consumption for the device, which reduces its stability and service life [4,5]. Therefore, it is of great significance to study a highly sensitive sensor for detecting NO_2 gas at room temperature.

Graphene exhibits a perfect two-dimensional crystal structure, single atomic layer thickness and high conductivity, which enables it to reach the level of detecting a single NO_2 gas molecule [6,7]. Studies have found that GO has excellent gas-sensing properties [8,9]; this is because GO is an important derivative of graphene. It has properties similar to graphene and its surface contains oxygen-containing functional groups such as hydroxyl, carboxyl, epoxy and carbonyl [10]. In addition, rGO can be obtained by reduction treatment of GO, and a gas sensor based on such a material can work at room temperature [11,12]. The structural defects generated by the reduction process can enhance the gas-sensing properties of rGO to a certain extent. Chemical reduction by hydrazine hydrate is a common and simple method. Lu [13] found that rGO showed a good response to low concentration NO_2 (2 ppm) and NH_3 (1%) at room temperature, with a sensitivity of 12% and a response time of 40 min. To improve the sensor sensitivity and response recovery time, Zhang [14] prepared a NO_2 sensor based on a rGO/SnO_2 composite material. In an environment containing 5 ppm of NO_2, the response was found to be 3.13 at a test temperature of 50 ℃. Gu [15] prepared an NO_2 sensor based on a rGO/In_2O_3 composite material. In an environment containing 30 ppm of NO_2, the sensor showed a response of 8.25, response time of 4 min, and a recovery time of 24 min. At present, there are many reports for research into the chemical reduction GO, but there are significant differences in the oxygen-containing functional groups, structures and properties of rGO prepared with varying hydrazine dosage. Moreover, there are few reports in related literature, and the changes in the rGO structure and their influence on the gas-sensing properties of NO_2 need to be further studied.

In this paper, graphite oxide powder was prepared using the improved Hummers method and a graphite oxide sol was prepared by an ultrasonic dispersion method. Under the condition of a varying dosage of hydrazine, the GO sol was reduced to different degrees of reduction for rGO. A variety of characterization methods, such as XRD, Raman, FT-IR and a sensor test (WS-30 A), were used to reveal the dosage of the hydrazine GO structure, the influence of the oxygen-containing functional group on gas-sensing properties and the inherent law.

2. EXPERIMENTAL

2.1. Materials, reagents and devices

Materials: Ultra-fine-scale graphite (carbon content≥ 99.9%, -200 mesh, nanshu graphite mine).

Reagents: H_2SO_4 (95.0-98.0% concentration, analysis of pure), $KMnO_4$ (the purity≥99.5%, analysis of pure), H_2O_2 (the purity≥30%, analysis of pure), concentrated HCl (concentration of 36.0 ~ 38.0%, and analytical pure), ammonia water (pH =11, the purity≥96%), deionized water (>10 MΩ·cm), hydrazine hydrate ($H_4N_2·H_2O$, the purity≥80%) and high purity NO_2 (the purity≥99.5%).

Devices: Integrated program-controlled high temperature furnace (sxc-5-16); Electronic balance (JT2003 type), vacuum pump (SHZ-D (III) type), thermostatic drying oven (202-1 type),

ultrapure water system (while UPT-II-10 t), ultrasonic cleaners (KQ5200DE), water bath pot, mixer, digital pH meter, centrifuge, digital multimeter, self-assembly resistance temperature, WS-30A type a gas sensor test equipment.

2.2. Material Synthesis

Preparation of GO: graphite oxide was prepared by using the improved Hummers method [16]. In particular, 25 mL 98% H_2SO_4 and 1 g ultra-fine-flake graphite was added to a beaker in turn and stirred in an ice bath for 30 min to ensure thorough mixing. Then, 3 g of KMnO4 was weighed out and slowly added into the beaker mixture, which was continuously stirred for 120 min in a thermostatic water bath at 35℃. Then, deionized water was added to the reaction solution, and the reaction carried out at 80℃ for 13 min. Next, H_2O_2 with a concentration of 5% was added to the system until no gas was generated, followed by filtering of the solution while it was still hot. Finally, the sample was thoroughly washed with 5% dilute HCl and deionized water until a neutral filtrate was obtained. The graphite oxide sample was prepared by drying the filter paper at 60 ℃ for 24 h. Then, 0.3 g of the prepared graphite oxide was added into a beaker containing 100 mL ammonia solution with pH=11. The solution was treated with ultrasound for 2 h. After washing and centrifugation, a GO aqueous dispersion solution with a concentration of 3 mg/mL was obtained.

Preparation of GO at different reduction levels: 0.05 mL, 0.1 mL, 0.2 mL, 0.5 mL and 1 mL hydrazine hydrate was added into a beaker containing a 100 mL homogeneous stable GO suspension; the above mixture was then placed under the condition of a 90 ℃ water bath pot for 2 h. The obtained different reduction degrees for the graphene oxide colloidal suspension were labeled as rGO-0.05, rGO-0.1, rGO-0.2, rGO-0. 5, and rGO-1.

Preparation of the gas sensing elements: samples obtained from the reduction treatment at varying levels of hydrazine hydrate dosage were taken with a pipette, 20 μL, and uniformly coated onto a Ag-Pd interdigital electrode substrate, placed in an oven, dried at 60℃ for 30 min, and then coated three times after removal. Gas sensing elements based on rGO with different degrees of reduction were prepared. The number was the same as above. The sample preparation and testing process are shown in Fig. 1.

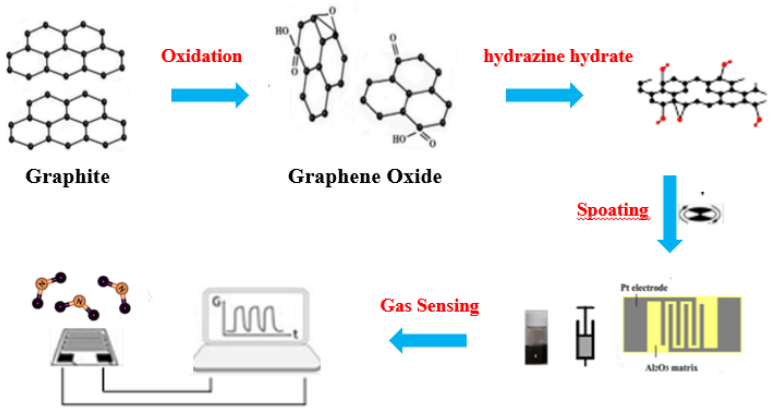

Figure 1. Schematic illustration for synthesis and gas-sensing of the rGO

2.3. Characterization.

XRD analysis was carried out with an X′ Pert MPD Pro X-ray diffractometer produced by the Panaco company in the Netherlands using a Cu target, emission slit (DS) : (1/2) °, antiscattering slit (SS) : 0.04 °, reception slit (AAS) : 5.5 nm, scanning range: 3°-80°. FT-IR analysis was carried out using a Nicolet-5700 infrared spectrometer produced by Nigri. The scanning wavenumber range was 4000-400 cm^{-1}. Raman analysis was performed with an InVir laser Raman spectrometer manufactured by Renisaw.

The resistance-temperature curve test procedure involved placing the gas sensor onto a heating plate and setting the maximum heating temperature to 80℃. In the process of heating/cooling, the resistance value of the gas sensor was recorded at 5℃ intervals and tested 3 times.

The gas-sensing properties test adopted a WS-30A gas-sensing element tester produced by the ZhengZhou WeiSheng instrument company. The number of test channels was 30; the acquisition speed was 1 time/second. The test voltage was 5 V DC and the system comprehensive error was < ± 1%.

3. RESULTS AND DISCUSSION

3.1. Appearance characteristics.

Fig. 2 shows the SEM images of GO and rGO-x (x=0.05 mL, 0.1 mL, 0.2 mL, 0.5 mL, and 1 mL) samples. It can be seen that GO shows obvious banded folds, which are caused by the uneven dispersion of the GO solution. When 0.05 ml hydrazine hydrate was added, rGO-0.05 presented a transparent film; this was because the addition of hydrazine hydrate resulted in an increase in pH value for the GO solution and better dispersibility. As the amount of hydrazine hydrate increased (0.1 mL, 0.2 mL, 0.5 mL and 1 mL), the sample morphology became more uniform and transparent.

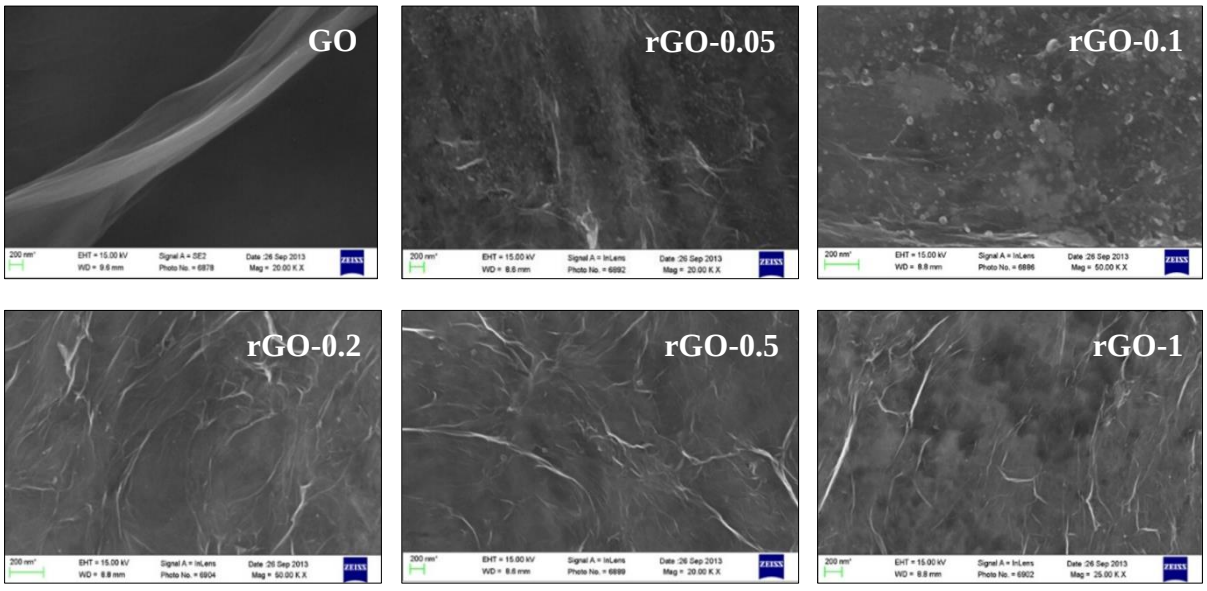

Figure 2. SEM images of GO, rGO-0.05, rGO-0.1, rGO-0.2, rGO-0.5 and rGO-1 samples

3.2. Structural features

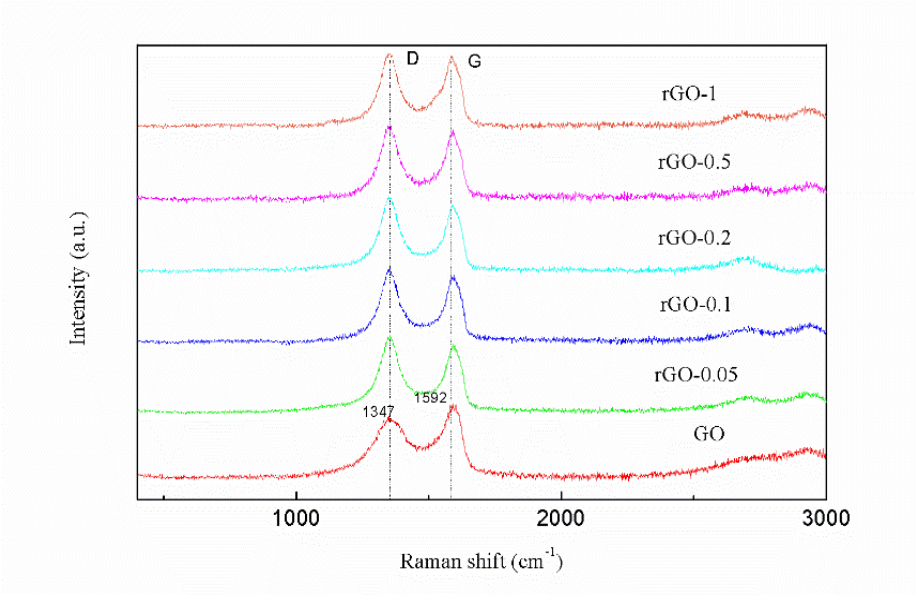

Figure 3. Raman pattern of GO, rGO-0.05, rGO-0.1, rGO-0.2, rGO-0.5 and rGO-1 samples

Fig. 3 shows a Raman diagram for the GO and samples rGO-x (x = 0.05 mL, 0.1 mL, 0.2 mL, 0.5 mL and 1 mL). It can be seen that each sample shows two similar characteristic peaks: D peak due to defects near 1350 cm^{-1} and a G peak due to the E_{2g} vibration at 1597 cm^{-1}. Generally, the ratio of the integral area of peak D and peak G (I_D/I_G) can be used to represent the defect and disorder degree of the structure. The larger the I_D/I_G value, the more defects in the structure and the greater the degree of disorder [17,18].

Table 1 shows the parameters obtained after fitting the D and G peaks for the sample using a Lorenz method. It can be seen that for a hydrazine hydrate dosage of 0.05 ml, compared with the GO sample, the G peak is shifted to a higher wavenumber, and the I_D/I_G is increased. As the amount of hydrazine hydrate increases (0.1 mL, 0.2 mL, 0.5 mL and 1 mL), the I_D/I_G ratio for the sample decreased.

Table 1. Raman parameters of GO and rGO-x samples

Sample	D-band/cm^{-1}		G-band/cm^{-1}		I_D/I_G	L_a/nm
	Raman shift	FWHM	Raman shift	FWHM		
GO	1358.39	154.55	1587.96	80.55	1.549	28.41
rGO-0.05	1352.29	108.54	1592.80	72.79	1.592	28.64
rGO-0.1	1352.50	98.84	1592.21	74.19	1.407	31.26
rGO-0.2	1352.33	94.86	1591.10	68.26	1.493	29.47
rGO-0.5	1352.14	90.08	1589.51	71.77	1.328	33.14
rGO-1	1350.90	88.84	1585.56	74.83	1.219	36.10

This is mainly related to the increase in the area of the sp^2 hybrid region after reduction, the average size of the graphene crystal plane, and the periodicity of the arrangement of carbon atoms. As

the amount of hydrazine hydrate continues to increase, the oxygen-containing functional groups on the surface of GO decrease, the number of defects decreases, and the degree of disorder is restored, the I_D/I_G ratio gradually decreases, and the relative scale of the graphene sheet layer L_a increases.

3.3. Functional group characteristics

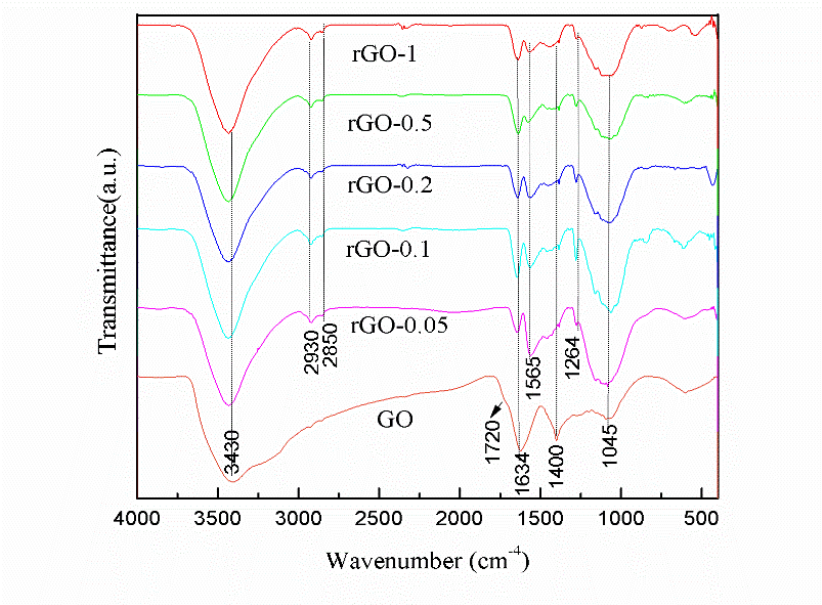

Figure 4. FT-IR spectra of the GO, rGO-0.05, rGO-0.1, rGO-0.2, rGO-0.5 and rGO-1 samples

Fig. 4 shows the characteristics of the FT-IR spectra obtained for GO and rGO-x samples (x = 0.05 mL, 0.1 mL, 0.2 mL, 0.5 mL and 1 mL). It can be seen that the GO structure contains oxygen-containing functional groups such as hydroxyl, epoxy and carboxyl groups. The number of oxygen-containing functional groups gradually decreases as the amount of hydrazine hydrate increases. Among these functional groups, the C=O vibration at 1720 cm^{-1} and the absorption peak due to C-O-C at 1264 cm^{-1} disappeared completely when the amount of hydrazine hydrate was increased to 1 mL. The peak approximately 1565 cm^{-1} was attributed to the C=C telescopic vibration peak, which recovered gradually with increasing hydrazine hydrate dosage. This indicated that the amount of hydrazine hydrate had a significant effect on the functional group content and that the reduction degree for GO gradually increased with increasing amount of hydrazine hydrate.

3.4. Resistance temperature characteristics

Fig. 5 shows the resistance-temperature curve for GO and rGO-x samples (x = 0.05 mL, 0.1 mL, 0.2 mL, 0.5 mL and 1 mL). It can be seen that the resistance of rGO-0.05, rGO-0.1, rGO-0.2, rGO-0.5 and rGO-1 decreased with increasing test temperature. This is because the test temperature increased, and more electrons in the valence band gained energy and entered the conduction band due to the thermal excitation, which enhanced the conductivity and reduced the resistance [19, 20]. With

increasing amount of hydrazine hydrate, the sample resistance was measured to be 645 KΩ, 13.3 KΩ, 8.9 KΩ, 5.4 KΩ and 4.9 KΩ with a decreasing trend, indicating that with the increase in the amount of hydrazine hydrate, the degree of GO reduction increased, the number of oxygen-containing functional groups decreased in great quantities, the sp^2 hybridization region was largely recovered and π electron concentration increased [21, 22]. This is consistent with the analysis results obtained from FT-IR and Raman.

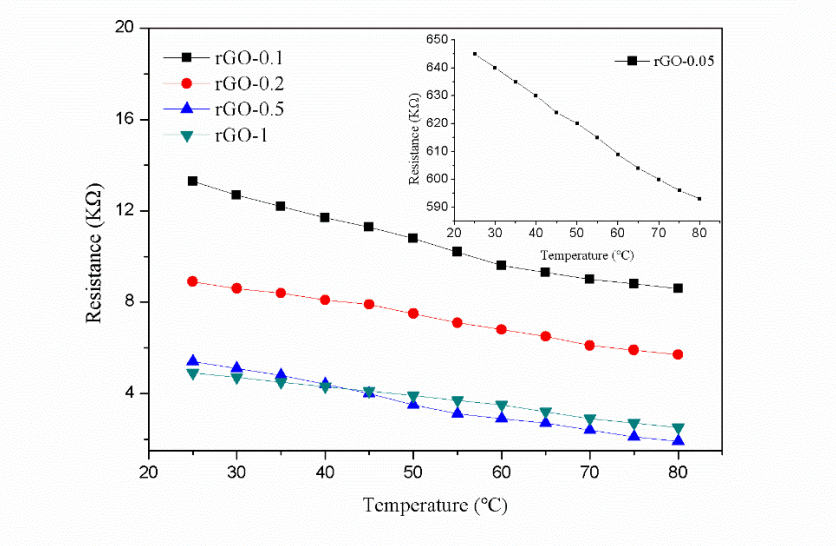

Figure 5. Resistance-temperature curve of the rGO-0.05, rGO-0.1, rGO-0.2, rGO-0.5 and rGO-1 samples

3.5. Gas-sensitivity performance

3.5.1 Static response

Sensitivity was defined as S=ΔR/R*100%, where R is the stable resistance value in an air environment, and ΔR is the resistance difference for the gas at room temperature. Fig. 6 shows the sensitivity to concentration relation curves for rGO-x (x=0.05 mL, 0.1 mL, 0.2 mL, 0.5 mL and 1 mL) treated with different levels of hydrazine hydrate dosage. It can be seen that the corresponding static sensitivity of the sample increases with increasing NO_2 concentration; among which, changes in the sensitivity for rGO-0.1 are the most obvious, while rGO-0.3, rGO-0.5 and rGO-1 show no significant change. At room temperature, the sensitivity of rGO-0.05, rGO-0.1, rGO-0.2, rGO-0.5 and rGO-1 was determined to be 31.47%, 42.17%, 20.23%, 18.65% and 17.01%, respectively, at a NO_2 concentration of 100 ppm. This is because GO is able to disperse stably under alkaline conditions and has oxidizing properties, while hydrazine hydrate is a strong reducing agent and can react with oxygen-containing functional groups (-OH, -O-, -COOH, etc.) contained in the GO structure under certain conditions [23]. As the amount of hydrazine hydrate increases, the degree of reduction also increases, reducing the sensitivity of the sample to NO_2. Therefore, the sensitivity characteristics of rGO-0.1 are better than that of rGO-0.2, rGO-0.5 and rGO-1.

It can also be seen that there is an almost linear relationship between the responsiveness and NO_2 concentration. The linear function of the relationship between the responsiveness and NO_2 concentration can be expressed as follows: y=0.40572X+4.778, where X stands for the concentration of NO_2 and y stands for the responsiveness.

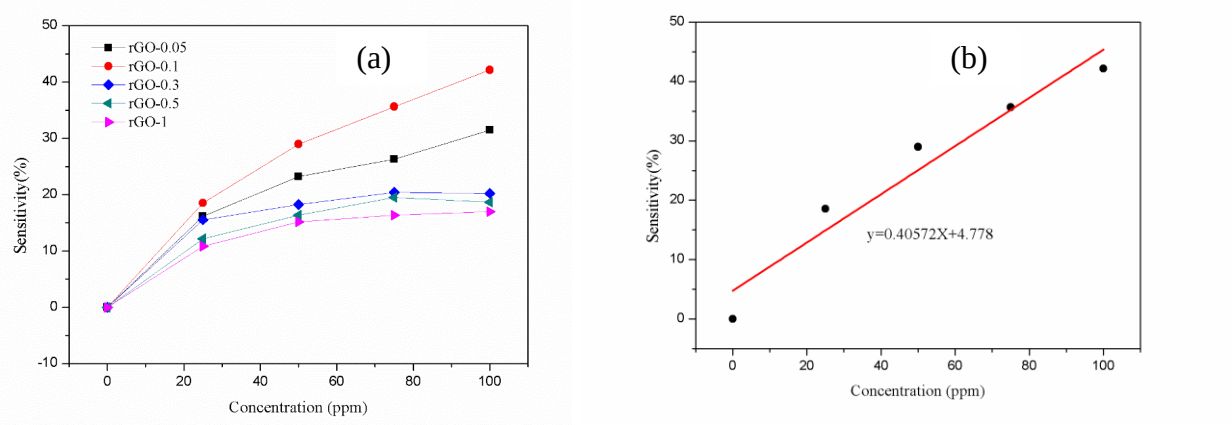

Figure 6. Static response Curves, (a)the sensitivity curves of relationship of sample rGO-x at different NO_2 concentrations, (b) the relationship between the concentration and the sensitivity of GO-0.1

3.5.2 The dynamic response

Fig. 7 shows the response and recovery time for the rGO-0.05 and rGO-0.1 samples at room temperature with a NO_2 concentration of 100 ppm. The response time can describe the time required for NO_2 molecular adsorption, and the recovery time is the time required to describe stripping of NO_2 molecules. Usually, the response and recovery time can be defined as the resistance value Δ R*60%.

It can be seen that when the sample is exposed to NO_2, the sample resistance tends to decrease. This is because when NO_2 molecules are adsorbed onto the surface of the material, charge transfer occurs between the NO_2 molecules and the gas-sensitive material, resulting in a lower resistance [24]. When the NO_2 exposure was stopped and clean air was used for recovery, the resistance showed a slowly rising upward trend, but failed to return to the initial value, which was mainly due to the incomplete desorption of NO_2 [25]. As the concentration of NO_2 increases, more NO_2 molecules are adsorbed onto the surface of rGO. Accordingly, more gas molecules will remain on the surface of rGO during desorption, resulting in a longer recovery time. For a hydrazine hydrate dosage of 0.1 ml, the oxygen-containing functional groups on the GO surface are almost completely eliminated, mainly due to absorption of NO_2 by the active C atoms at the edge of the defect, from which NO_2 desorption is difficult [26]. However, with increasing time, the gas molecules at each adsorption site will gradually desorb, resulting in a longer recovery time.

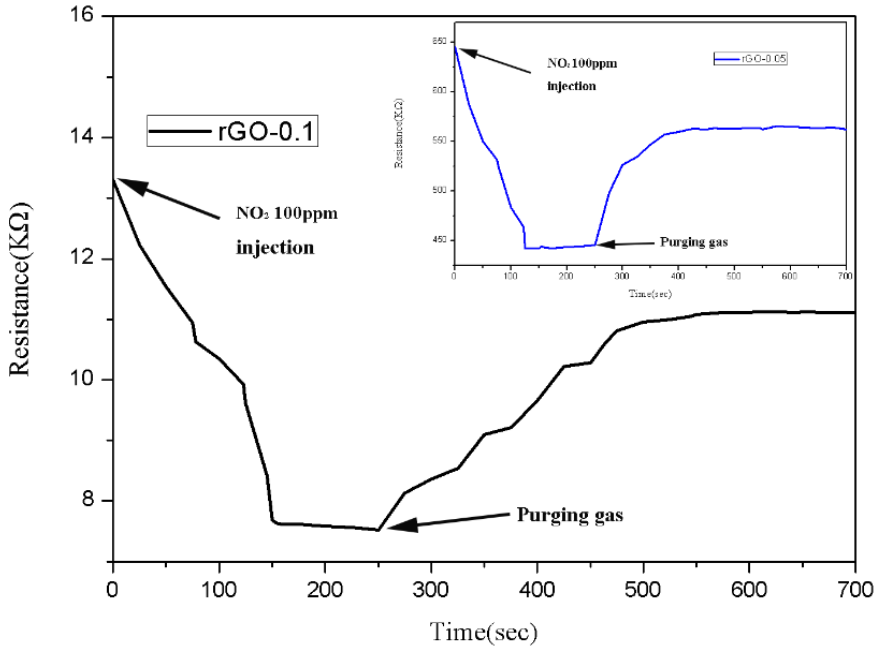

Figure 7. Dynamic response curves of rGO-0.1 at 100ppm NO_2 concentration. The inset shows the dynamic response curves of rGO-0.05 at 100ppm NO_2 concentration

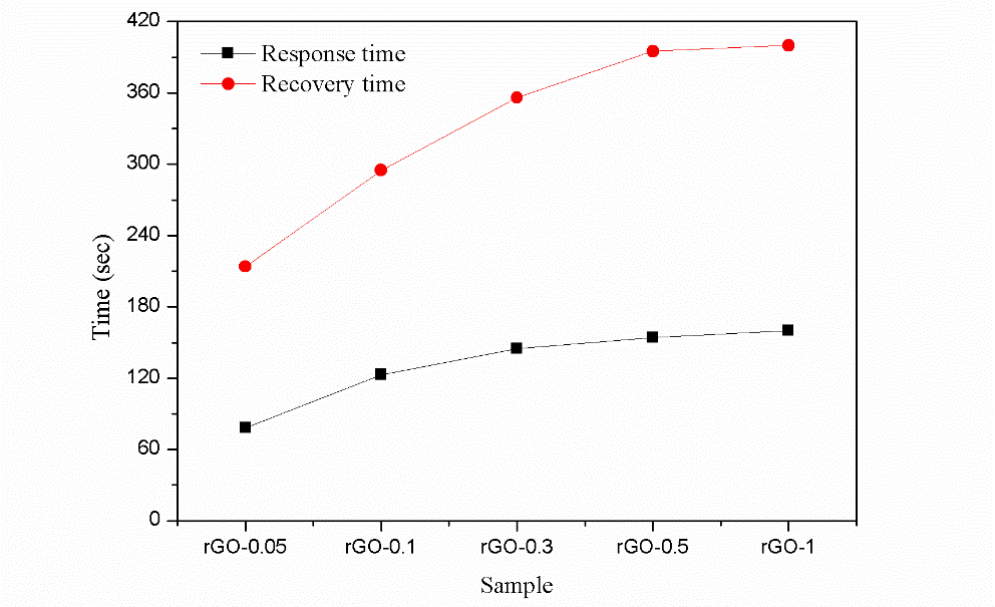

Figure 8. Response - recovery time curve of rGO-0.05, rGO-0.1, rGO-0.2, rGO-0.5 and rGO-1 samples at 100ppm NO_2 concentration

Fig. 8 shows the response-recovery time curve at 100 ppm for rGO-x samples (x = 0.05 mL, 0.1 mL, 0.2 mL, 0.5 mL and 1 mL) treated with different amounts of hydrazine hydrate. It can be seen that with increasing hydrazine hydrate dosage, both the response time and recovery time for the sample gradually increase. The response time is approximately 78 s, 123 s, 145 s, 154 s and 160 s and the recovery time is 214 s, 295 s, 356 s, 395 s and 400 s, respectively. This is because the number of

oxygen-containing functional groups in the highly reduced graphene oxide is very small, which reduces the sensitivity to NO_2. In particular, the sample (rGO-1) with a high degree of reduction finds it difficult to recover to the initial state at room temperature.

Table 2 shows a comparative analysis of the sensitivity of different graphene materials to NO_2 gas. It can be seen that the results from this study show a faster response characteristic, and the response time of NO_2 at 100 ppm is 123 s. The rGO in this work has a fast response without requiring external energy injection, but the recovery ability needs to be further improved.

Table 2. Graphene based gas sensors for NO_2 detection

Properties of sensing material	Test gas(ppm)	Gas response	Response time	Recovery time	Ref.
rGO	2	1.56（Gg-Ga）/ Ga	~30min	> 30min	[13]
3D graphene/rGO	100	1.079(Ra/Rg)	> 310s	373s	[27]
rGO	4.5	20%($\Delta R/R_0$)	> 300s	> 300s	[28]
CVD graphene	10	15%($\Delta R/R_0$)	~30min	~45min	[29]
Graphene	15	7.5%（Gg-Ga）/ Ga	~7.5min	~17min	[30]
This work	100	42.7%（$\Delta R/R$）	123s	295s	

3.6. Mechanism analysis

The main reason for rGO showing excellent gas-sensitivity to NO_2 is that when rGO adsorbs NO_2 molecules, the Fermi level of rGO changes, and charge transfer can occur directly between the molecules [31]. According to Mulliken population analysis, the NO_2 molecule obtains a charge of 0.196e from graphene [24]. The conductivity of graphene can be expressed as:

$$\sigma = ne\mu$$

where n, e and μ represent the carrier concentration, charge of the electron, and carrier migration rate, respectively. Therefore, the conductivity of graphene is not only affected by the carrier mobility at the Fermi energy level but also related to the carrier concentration. Studies have shown that rGO exhibits typical p-type semiconductor properties [32], while NO_2 as an oxidizing gas acts as an electron acceptor, so the adsorption of NO_2 gas can lead to enhancement of the hole density and conductivity of rGO, thereby improving the gas sensitivity. On the other hand, due to incomplete reduction, hydroxyl and epoxy groups remain on the surface of rGO, which is conducive to the adsorption of gas molecules. At the same time, the reduction reaction will further introduce vacancies and structural defects, providing more reaction sites, and helping one to further adsorb gas molecules [33]. Based on the above reasons, rGO reduced by hydrazine hydrate shows a very excellent gas-sensing performance.

The experimental results show that as the NO_2 gas concentration increases, the rGO resistance gradually decreases. The main reason for this is that charge-induced charge transfer will lead to a

decrease in the rGO resistance; the resistance value decreases gradually, and the sensitivity also increases. In addition, the electrostatic potential of the atoms on the adsorption surface will increase significantly after the gas is adsorbed [34], resulting in a decrease in resistance. Furthermore, NO_2 is a magnetic molecule, and the adsorption of rGO will lead to a change in the magnetic state of NO_2, resulting in a change in the density of the states for the system, resulting in a change in the electronic properties of the rGO adsorption system, which in turn will lead to a change in resistance [35].

4. CONCLUSIONS

rGO-x samples with different degrees of reduction were obtained by controlling the amount of hydrazine hydrate and characterized by SEM, Raman and FT-IR. Meanwhile, the NO_2 sensitivity for the as-prepared rGO-x samples was tested and the following conclusions were drawn:

(1) As the amount of hydrazine hydrate increases, the sample I_D/I_G ratio gradually decreases, indicating that the area of the sp^2 hybrid orbital increases after reduction, the average size of the graphene crystal plane increases, the arrangement of carbon atoms increases periodically, and the structure gradually approaches that of the graphene structure. For a hydrazine hydrate amount of 0.1 mL, the reduction is basically complete.

(2) As the amount of hydrazine hydrate increases, the sensitivity shows a decreasing trend, while the response-recovery time shows an increasing trend. In an environment with a NO_2 concentration of 100 ppm, the response time for the rGO-0.05, rGO-0.1, rGO-0.2, rGO-0.5 and rGO-1 samples was determined to be approximately 78 s, 123 s, 145 s, 154 s and 160 s, respectively. The recovery time for the sample samples was determined to be 214 s, 295 s, 356 s, 395 s and 400 s, respectively.

(3) In contrast, rGO-0.1 shows a very high gas sensitivity to NO_2. Under an environment containing 100 ppm NO_2, the rGO-0.1 sample showed a static response sensitivity of 42.17%, response time of 123 s, and a recovery time of 295 s.

References

1. A.K. Geim, *Science*, 324 (2009) 1530.
2. G. Ou, P.X. Fan, H.J. Zhang, K. Huang, C. Yang, W. Yu, H.H. Wei, M.L. Zhong, H. Wu, Y.D. Li, *Nano Energy*, 35 (2017) 207.
3. Y.H. Navale, S.T. Navale, N.S. Ramgir, F.J. Stadler, S.K. Gupta, D.K. Aswal, V.B. Patila, *Sens. Actuators, B*, 251 (2017) 551.
4. S.J. Park, J. Park, H.Y. Lee, S.E. Moon, K.H. Park, J. Kim, S. Maeng, F. Udrea, W.I. Milne, G.T. Kim, *J. Nanosci. Nanotechnol*., 10 (2010) 3385.
5. H. Chen, T.J. Peng, B. Liu, H.J. Sun, *Mater. Rep*, 30 (2016) 57.
6. F. Schedin, K.S. Novoselov, S.V. Morozov, *Nat. Mater.*, 6 (2006) 652.
7. J. Sun, M. Muruganathan, H. Mizuta, *Sci. Adv.*, 2 (2016) 1.
8. M.G. Chung, D.K. Kim, H.M. Lee, T. Kim, J.H. Choi, D. Seo, J. B. Yoo, S.H. Hong, T.J. Kang, Y.H. Kim, *Sens. Actuators, B*, 166 (2012) 172.
9. J.D. Fowler, M.J. Allen, V.C. Tung, *ACS Nano*, 3 (2009) 301.

10. G. Venugopal, K. Krishnamoorthy, R. Mohan, *Mater. Chem. Phys.*, 132 (2012) 29.
11. J.L. Cao, Q. Cong, Y. Wang, Z.Y. Zhang, *Eur. J. Lipid Sci. Technol.*, 11 (2015) 32.
12. A. Lipatov, A. Varezhnikov, P. Wilson, V. Sysoev, A. Kolmakov, A. Sinitskii, *Nanoscale*, 5 (2013) 5426.
13. G. Lu, L.E. Ocola, J. Chen, *Nanotechnology*, 20 (2009) 1.
14. H. Zhang, J. Feng, T. Fei, *Sens. Actuators, B*, 190 (2014) 472.
15. F.B. Gu, R. Nie, D.M. Han, Z.H. Wang, *Sens. Actuators, B*, 219 (2015) 94.
16. Y.H. Yang, H.J. Sun, T.J. Peng, *Acta Phys-Chim. Sin.*, 27 (2011) 736.
17. J.D. Wang, T.J. Peng, H.J. Sun, *Acta Phys-Chim. Sin.*, 30 (2014) 2077.
18. A.C. Ferrari, *Solid State Commun.*, 143 (2007) 47.
19. D. Shang, L.B. Lin, J. He, *Journal of Sichuan University (Natural Science Edition)*, 42 (2005) 523.
20. J. Wu, W. Pisula, K. Müllen, *Chem. Rev.*, 107 (2007) 718.
21. L.F. Qiu, H.Y Zhang, W.G.Wang, Y.M. Chen, R. Wang, *Appl. Surf. Sci.*, 319 (2014) 339.
22. Y.Q. Feng, J.P. Zhao, X.B.Yan, F.L.Tang, Q.J. Xue, *Carbon*, 66 (2014) 334.
23. L. Guo, X.K. Chen, X.L. Wang, *Vacuum and Cryogenics*, 20 (2014) 38.
24. C.L. Cen, Z.Q. Chen, D.Y. Xu, L.Y. Jiang, X.F. Chen, Z. Yi, P.H. Wu, G.F. Li, Y.G. Yi, *Nanomaterials*, 10 (2020) 95.
25. D.W. Boukhvalov, M.I. Katsnelson, *J. Am. Chem. Soc.*, 130 (2008) 10697.
26. Y.H. Zhang, Y.B. Chen, K.G. Zhou, *Nanotechnology*, 20 (2009) 5504.
27. L. Li, S. He, M. Liu, C. Zhang, W. Chen, *Anal. Chem.*, 87 (2015) 1638.
28. Y.J. Yun, W.G. Hong, N.J. Choi, H.J. Park, S.E. Moon, B.H. Kim, K.B. Song, Y. Jun, H.K. Lee, *Nanoscale*, 6 (2014) 6511.
29. A. Zandiatashbar, G.H. Lee, S.J. An, S. Lee, N. Mathew, M. Terrones, T. Hayashi, C.R. Picu, J. Hone, N. Koratkar, *Nat. Commun.*, 5 (2014) 1.
30. A.K. Singh, M.A. Uddin, J.T. Tolson, H. Maire-Afeli, N. Sbrockey, G.S. Tompa, M.G. Spencer, T.Vogt, T.S. Sudarshan, G. Koley, *Appl. Phys. Lett.*, 102 (2013) 043101.
31. M.G. Chung, D.H. Kimb, H.M. Lee, T. Kim, J.H. Choi, D.K. Seo, J.B. Yoo, S.H. Hong, T. J. Kang, Y.H. Kim, *Sens. Actuators, B*, 166 (2012) 172.
32. J.W. Wang, Y. Kwak, I. Lee, S. Maeng, G.H. Kim, *Carbon*, 11 (2012) 50.
33. C. Li, L. Cai, W.W. Li, D. Xie, B.J. Liu, L. Xiang, X.K. Yang, D.N. Dong, J.H. Liu, C. Li, B. Wei, *Acta Phys. Sin.*, 68 (2019) 118102.
34. B. Cho, M.G. Hahm, M. Choi, J. Yoon, A.R. Kim, Y.J. Lee, S.G. Park, J.D. Kwon, C.S. Kim, M. Song, Y. Jeong, K.S. Nam, S. Lee, T.J. Yoo, C.G. Kang, B.H. Lee, H.C. Ko, P.M. Ajayan, D.H. Kim, *Sci. Rep.*, 5 (2015) 8052.
35. C. Jin, X. Tang, X. Tan, S.C. Smith, Y. Dai, L.Z. Kou, *J. Mater. Chem. A*, 7 (2019) 1099.